

# Tracer diffusion in F-actin and Ficoll mixtures

## Toward a model for cytoplasm

Li Hou,\* Frederick Lanni,<sup>†</sup> and Katherine Luby-Phelps<sup>§</sup>

Center for Fluorescence Research in Biomedical Sciences, and Departments of \*Physics, <sup>†</sup>Biology, and <sup>§</sup>Chemistry, Carnegie Mellon University, Pittsburgh, Pennsylvania 15213 USA

**ABSTRACT** We have previously reported that self-diffusion of inert tracer particles in the cytoplasm of living Swiss 3T3 cells is hindered in a size-dependent manner (Luby-Phelps, K., D. L. Taylor, and F. Lanni. 1986. *J. Cell Biol.* 102:2015–2022; Luby-Phelps, K., P. E. Castle, D. L. Taylor, and F. Lanni. 1987. *Proc Natl. Acad. Sci. USA.* 84:4910–4913). Lacking a theory that completely explains our data, we are attempting to understand the molecular architecture responsible for this phenomenon by studying tracer diffusion in simple, reconstituted model systems. This report contains our findings on tracer diffusion in concentrated solutions of Ficoll 70 or Ficoll 400, in solutions of entangled F-actin filaments, and in solutions of entangled F-actin containing a background of concentrated Ficoll particles or concentrated bovine serum albumin (BSA). A series of size-fractionated fluorescein-Ficolls were used as tracer particles. By fluorescence recovery after photobleaching (FRAP), we obtained the mean diffusion coefficients in a dilute, aqueous reference phase ( $D_0$ ), the mean diffusion coefficients in the model matrices ( $D$ ), and the mean hydrodynamic radii ( $R_H$ ) for selected tracer fractions. For each model matrix, the results were compared with similar data obtained from living cells. As in concentrated solutions of globular proteins (Luby-Phelps et al., 1987),  $D/D_0$  was not significantly size-dependent in concentrated solutions of Ficoll 400 or Ficoll 70. In contrast,  $D/D_0$  decreased monotonically with increasing  $R_H$  in solutions of F-actin ranging in concentration from 1 to 12 mg/ml. This size dependence was most pronounced at higher F-actin concentrations. However, the shape of the curve and the extrapolated value of  $D/D_0$  in the limit,  $R_H \rightarrow 0$  did not closely resemble the cellular data for tracers in the same size range ( $3 < R_H < 30$  nm). In mixtures of F-actin and Ficoll or F-actin and BSA,  $D/D_0$  was well approximated by  $D/D_0$  for the same concentration of F-actin alone multiplied by  $D/D_0$  for the same concentrations of Ficoll or BSA alone. Based on these results, it is possible to model the submicroscopic architecture of cytoplasm in living cells as a densely entangled filament network (perhaps made up of F-actin and other filamentous structures) interpenetrated by a fluid phase crowded with globular macromolecules, which in cytoplasm would be primarily proteins.

## INTRODUCTION

The aqueous matrix that surrounds and contains the formed elements of the cytoplasmic space is often referred to as the “cytosol” (Lardy, 1965; Anderson and Green, 1967; Clegg, 1984). However, it is inaccurate to regard the cytoplasmic matrix as a simple fluid, despite the fact that it is 75–80% water by weight (De Robertis et al., 1970). In fact, bulk cytoplasm is ~20% protein (Lanni et al., 1985; Fulton, 1982), and has the physical properties of a weakly viscoelastic gel (e.g., Conklin, 1940; Marsland, 1942; Frey-Wyssling, 1953; Allen, 1961; Pollard, 1984; Porter, 1984; Stossel et al., 1985; Taylor and Condeelis, 1979; Taylor and Fehcheimer, 1982). Morphological and biochemical evidence suggests this gel is made up of a network of cytoskeletal filaments, among which the muscle microfilament protein, F-actin, appears to be the most prominent (Allen, 1961; Hartwig and Stossel, 1979;

Taylor and Fehcheimer, 1982; Pollard, 1984; Woloszewick and Porter, 1979; Schliwa and Van Blerkom, 1981).

Until recently, it has been difficult to test this hypothesis in living cells. Optical microscopy is the tool best suited to the study of living cells, but the resolution of traditional optical microscopic methods is not sufficient to obtain information at the molecular level. The technique of fluorescence recovery after photobleaching (FRAP) (Wolf, 1989) offers a means of testing the hypothesis by studying the long-range diffusion of inert, fluorescent tracer particles in the cytoplasm of living cells.

Tracer diffusion is an established means of probing the submicroscopic architecture of complex polymer matrices (Laurent, 1967; Laurent and Granath, 1967; Deen et al., 1981; Sellen, 1983; Phillies, 1987). Data are commonly presented in terms of  $D_0$ , the diffusion coefficient of the tracer in a reference phase;  $D$ , the diffusion coefficient of the tracer in the matrix;  $D/D_0$ , the relative diffusion coefficient; and  $R_H$ , the hydrodynamic radius of the tracer. These parameters all can be obtained from FRAP

Address all correspondence to Dr. Luby-Phelps at her current address: Dept. of Physiology, The University of Texas Southwestern Medical Center at Dallas, 5323 Harry Hines Blvd., Dallas, TX 75235-9040.

data. The relationship of  $D/D_0$  to  $R_H$  depends on the architecture of the matrix in question. In a Newtonian fluid, tracer diffusion simply obeys the Stokes-Einstein equation  $D = kT/6\pi\eta R_H$ , where  $D$  is the diffusion coefficient and  $\eta$  is the fluid viscosity. Thus, if cytoplasm were a Newtonian fluid,  $D/D_0$  would be independent of  $R_H$ . In a more complex matrix, such as a gel network or a concentrated polymer solution, complicated excluded volume and hydrodynamic interactions of the tracer with the matrix may result in deviations from the Stokes-Einstein relationship. Several relevant theoretical treatments of this problem exist in the literature (Wang, 1954; Lauffer, 1961; Ogston et al., 1973; Cukier, 1984; Altenberger and Tirrell, 1984; Phillies, 1989).

In our studies we have used size-fractionated, fluorescein-Ficolls (FF) as tracer particles. FF are hydrophilic, have a low density of ionizable residues, and do not appear to bind with high affinity to intracellular components (Luby-Phelps et al., 1987). FF can be prepared as a series of fairly narrow size fractions by size-exclusion chromatography. Using dilute buffer solutions as a reference phase, we have found that  $D/D_0$  of FF fractions in the cytoplasm of living tissue culture cells is strongly size-dependent (Luby-Phelps et al., 1987), confirming that cytoplasm cannot be regarded as a simple Newtonian fluid. However, the observed dependence of  $D/D_0$  on  $R_H$  in the cytoplasm of living cells is not completely described by any of the published theories of long-range diffusion of tracers in gels or concentrated polymer solutions. Therefore, we have adopted an empirical approach to interpreting the cellular data in terms of the molecular architecture of cytoplasm by studying tracer diffusion in simple reconstituted systems. We have previously reported that  $D/D_0$  of FF diffusing in concentrated solutions of globular proteins is not significantly size-dependent (Luby-Phelps et al., 1987), suggesting that the high protein content of cytoplasm ( $\approx 20\%$ ) is not alone responsible for the strong size-dependence of  $D/D_0$  for FF diffusing in cells.

In the present study, we have attempted to model cytoplasm both as a network of entangled, uncross-linked filaments, and as an entangled filament network interpenetrated by a crowded background solution of globular macromolecules. For this purpose, we have studied FF diffusion in solutions of F-actin ranging from 1 to 12 mg/ml, and in solutions of F-actin containing high concentrations of nonfluorescent, unfractionated Ficoll 70 (F70) or Ficoll 400 (F400) or bovine serum albumin (BSA). For modeling cytoplasm simply as a three-component system of filaments, background spheres and solvent, Ficoll particles have advantages over proteins as background particles because their low surface-charge density prevents complications that might arise due to electrostatic interactions between proteins, and because

they are highly soluble in buffer solutions of widely varying ionic strength, even at concentrations as high as 30% by weight. Reports in the literature suggest that Ficoll particles have a well-defined size that is closely approximated by  $R_H$  (Deen et al., 1981). The sizes of particles found in unfractionated F70 and F400 ( $R_H = <1$  nm to  $\geq 30$  nm) span a range that includes cytoplasmic proteins. The use of Ficoll in our models is further justified by the observation that tracer diffusion in concentrated solutions of F70 or F400 resembles tracer diffusion in concentrated solutions of globular proteins, as will be described in Results.

## MATERIALS AND METHODS

### Reagents

Fluorescein isothiocyanate [FITC, isomer I], tris(hydroxymethyl)aminomethane [Tris], and bovine serum albumin [BSA] were obtained from Sigma Chemical Co., St. Louis, MO. Reagent-grade inorganic salts KCl, NaCl, CaCl<sub>2</sub>, and MgCl<sub>2</sub> were from J. T. Baker Chemical Co., Phillipsburg, NJ. Dithiothreitol [DTT] and disodium adenosine-5'-triphosphate [ATP] were from Boehringer-Mannheim Biochemicals, Indianapolis, IN. Sodium azide [NaN<sub>3</sub>] was from EM Science, Cherry Hill, NJ. Deionized distilled water was used in all buffer preparations. Bradford reagent was from Pierce Chemical Co., Rockford, IL.

### Preparation of fluorescein-Ficoll tracers

F400 (Pharmacia Fine Chemicals, Piscataway, NJ) was activated and labeled at low density with fluorescein isothiocyanate, as previously described (Luby-Phelps, 1989). The labeled polymers were fractionated by size exclusion chromatography on a  $5 \times 100$  cm column of Sepharose CL-6B (Pharmacia Fine Chemicals) in 10 mM Tris, 50 mM KCl, 0.02% NaN<sub>3</sub>, pH 8.0 at 20°C. Fractions of 4.5 ml were collected and stored in small aliquots at 4°C for short term use, or dialyzed in water, lyophilized, and stored at -20°C for later use. The mean  $D_0$  for each size fraction was obtained by FRAP (see below), and the mean hydrodynamic radius ( $R_H$ ) of each fraction was calculated from  $D_0$  by the Stokes-Einstein relation:  $R_H = kT/6\pi\eta D_0$ .  $R_H$  was found to range from 3 to 30 nm across the chromatogram.

### Actin preparation

Actin was extracted from an acetone powder of rabbit skeletal muscle according to the procedure of Spudich and Watt (1971). Monomeric actin (G-actin) was lyophilized with 2 mg sucrose per 1 mg actin and stored at -20°C. For use, G-actin was dissolved in buffer A (2 mM Tris, 0.2 mM CaCl<sub>2</sub>, 0.2 mM ATP, 0.2 mM DTT, 0.01% NaN<sub>3</sub>, pH = 8.0 at 4°C) and dialyzed at 4°C for 24 h with at least two exchanges of freshly made buffer A. The actin was then clarified by centrifugation at  $2 \times 10^5$  g for 2 h at 4°C. The supernatant, containing G-actin, was saved and the concentration of actin was determined from the difference in absorbance at 290 and 340 nm, using an extinction coefficient of  $E^{0.1\%} = 0.63$  (Houk and Ue, 1974). Actin prepared in this manner will be referred to as SW-actin. The actin concentrations used in our experiments ranged from 0 to 12 mg/ml. To achieve a concentration of 12 mg/ml, clarified, monomeric SW-actin was concentrated by vacuum dialysis in a 2-ml

collodion bag (Schleicher & Schuell, Inc., Keene NH) and then clarified again as above before use. Solutions remained optically clear during vacuum dialysis and no pellet was observed upon subsequent clarification, indicating that this treatment did not result in aggregation of actin monomers or denaturation of the protein.

For some experiments, SW-actin was further purified by size-exclusion chromatography in buffer A on a  $2 \times 40$ -cm column of Sephadex G-150 (Pharmacia Fine Chemicals) to remove capping proteins and small oligomers that could serve as nuclei for filament elongation. Two protein peaks in the eluate were detected by UV absorbance at 280 nm. The trailing fractions from the second peak contained no contaminants detectable by polyacrylamide gel electrophoresis. These fractions were pooled and used within 6 h to ensure the absence of nuclei. Actin prepared in this manner will be referred to as gel-filtered actin. The highest concentration of SW actin that could be achieved was 10–12 mg/ml, resulting in an upper limit of 1–2 mg/ml for the concentration of freshly gel-filtered actin.

## Ficoll solutions

Concentrated solutions of F400 and F70 (Pharmacia Fine Chemicals) were prepared by dissolving the powder directly in buffer A. For some experiments, concentrations as high as 30% (g/dl) were prepared to achieve the desired concentrations after mixing with G-actin solutions. The bulk shear viscosities of 6.9% F400, 7.7% F400, and 10.5% F70 in actin polymerization buffer were measured using a calibrated capillary viscometer (Cannon Instrument Co., State College, PA). All Ficoll concentrations reported here are in percentages (g/dl).

## Concentrated BSA solutions

BSA was dissolved in distilled water, dialyzed against distilled water, and lyophilized to produce a salt-free powder. The powder was dissolved in buffer A at a concentration of 23% before mixing with G-actin in buffer A. The shear viscosity of 7% BSA in actin polymerization buffer was measured as for Ficolls (above).

## Preparation of FRAP specimens

Stock solutions of FF, G-actin, and F70, F400 or BSA at known concentrations were prepared in buffer A. Aliquots of the stock solutions were diluted into buffer A to achieve the final concentration desired for each experiment. The final concentration of FF was always  $<0.1\%$ . Samples were brought up to their final volume by addition of concentrated KCl and  $\text{MgCl}_2$  to a final concentration of 100 mM KCl and 2 mM  $\text{MgCl}_2$ , and the sample was mixed by vortexing very briefly. Immediately after mixing, each sample was drawn into a flat borosilicate capillary tube with inner dimensions 0.1 mm deep  $\times$  0.8 mm wide  $\times$  50 mm long (No. 5010, Vitro Dynamics, Rockaway, NJ). Specimens were prepared on ice with all ingredients at  $\leq 4^\circ\text{C}$  to retard polymerization of actin so that samples could be drawn into the capillaries. The capillary was then mounted on a black-anodized aluminum plate and both ends of the capillary were sealed with Flo-Texx mounting medium (American Scientific Products, McGaw Park, IL). The most critical source of systematic error in our FRAP data was estimation of spot size, which was found to depend on daily variations in the adjustment of the FRAP instrument. To minimize this error, all FRAP measurements for each experiment were made in a single day. Because this often required up to 9 h, specimens were prepared and allowed to incubate at room temperature overnight in the dark, and measurements were made the next day. The diffusion data obtained from a given specimen 3 h after preparation were essentially the same as those measured after overnight

incubation at room temperature, showing that this procedure did not affect our results.

## Fluorescence recovery after photobleaching (FRAP)

Instrumentation and data analysis were as described by Simon et al. (1988a and b), with the following modifications. A beam expander and plano-convex lens were used to bring a laser beam through the epifluorescence excitation optics of the microscope to a focus at the specimen plane. Using a  $16\times$  objective lens, the fluorescent spot excited by the beam had a quasi-Gaussian intensity profile with a diameter of 20  $\mu\text{m}$  at the focal plane. An image-plane iris diaphragm was set to 3–4 beam diameters to minimize background scatter and noise by limiting detector field-of-view. Fluorescence intensity was measured by a photomultiplier (Hamamatsu Corp., Middlesex, NJ) input to an electrometer (model 602, Keithley Instruments, Inc., Cleveland OH). Data acquisition and analysis were controlled by an IBM PC-AT using ASYST software (Macmillan Software Co., New York, NY). The algorithm of Yguerabide et al. (1982) was used to obtain the diffusion coefficients and mobile fractions (% Rec, percentage fluorescence recovery) of the tracers from fluorescence recovery data. For each measurement, fluorescence recovery was monitored for at least 10 times the characteristic time constant, or recovery half-time,  $\tau$ . Reported diffusion coefficients and % Rec represent the mean of at least six measurements. The standard deviations were generally  $<5\%$  of the mean, and under optimal conditions were as low as 1.7% of the mean. All FRAP measurements were conducted at room temperature.

## RESULTS

### Tracer diffusion in F-actin solutions

Diffusion coefficients ( $D$ ) and % Rec of FF in solutions of F-actin at 1, 3, 5, 8, and 12 mg/ml were measured by FRAP.  $D_0$  and  $R_H$  were determined for each tracer size fraction as described in Materials and Methods. The relative diffusion coefficient,  $D/D_0$ , was found to decrease with tracer size ( $R_H$ ), as can be seen in Fig. 1a. This size dependence became more severe as the concentration of F-actin was increased from 1 to 12 mg/ml. Linear extrapolation of the  $D/D_0$  data to  $R_H = 0$  gives a value close to the inverse solvent viscosity (1.0 cP) for all actin concentrations used. (Deviations from 1.0 are due in part to systematic errors, which are the most significant source of uncertainty in these experiments). % Rec for all measurements of tracer diffusion in F-actin solutions was 100%, as shown in Fig. 1b. In addition, the observed diffusion coefficients for FF were always at least two orders of magnitude higher than diffusion coefficients reported for F-actin (Lanni and Ware, 1984; Tait and Frieden, 1982; Simon et al., 1988a). Together, these observations suggest that if any binding interaction exists between Ficoll and F-actin, it occurs as a fast-exchange process in which the tracer particles diffuse independently of the filaments (Elson and Qian, 1989).

Values of  $D/D_0$  essentially identical to those in 1

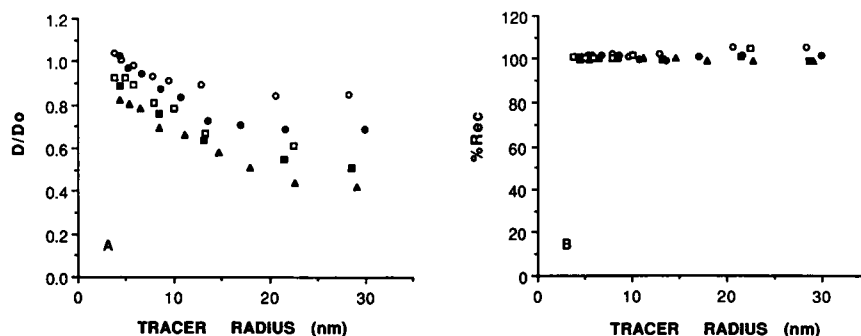


FIGURE 1 Relative diffusion coefficients ( $D/D_0$ ) and percentage mobile fractions (% Rec) for FF diffusing in several concentrations of F-actin, as a function of mean tracer radius ( $R_H$ ). (Open circles) 1 mg/ml actin; (solid circles) 3 mg/ml; (open squares) 5 mg/ml; (solid squares) 8 mg/ml; (solid triangles) 12 mg/ml. (A)  $D/D_0$  vs.  $R_H$ .  $D/D_0$  decreases with  $R_H$  and with F-actin concentration. At each F-actin concentration, a linear extrapolation to  $R_H = 0$  on the y-axis is  $\approx 1.0$ . (B) % Rec vs.  $R_H$ . No immobile fractions for FF diffusing in F-actin were detected, even at 12 mg/ml.

mg/ml polymerized SW-actin were obtained when FF diffusion was studied in solutions of polymerized gel-filtered actin at 1 mg/ml. Because it is difficult to make higher concentration solutions of freshly gel-filtered actin, all further experiments were performed using SW-actin.

### Tracer Ficoll diffusion in concentrated Ficoll or BSA solutions

Fig. 2 shows  $D/D_0$  of FF in solutions of F400, F70, or BSA as a function of  $R_H$ . The Ficoll concentrations tested were 10.4% F70, 6.9% F400, and 7.7% F400. The BSA concentration tested was 7.0%, determined refractometrically. In all cases,  $D/D_0$  showed only weak dependence on  $R_H$ . For a Newtonian fluid,  $D/D_0$  should equal the inverse relative viscosity,  $(\eta/\eta_0)^{-1}$ , where  $\eta_0$  denotes the viscosity of water at the same temperature. Table 1 shows that

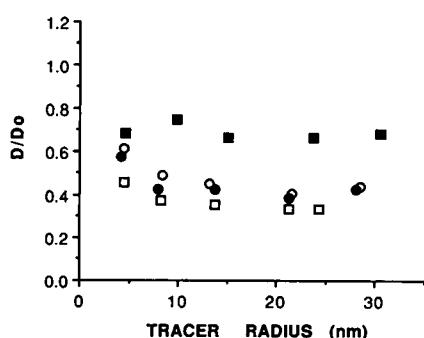


FIGURE 2 Relative diffusion coefficients ( $D/D_0$ ) of FF in concentrated solutions of Ficoll or BSA, as a function of mean tracer radius ( $R_H$ ). (Open circles) 6.9% F400; (solid circles) 7.7% F400; (open squares) 10.4% F70; (solid squares) 7.0% BSA.  $D/D_0$  shows weak size dependence over the size range used, asymptotically approaching the inverse relative viscosities  $(\eta/\eta_0)^{-1}$  of the solutions (see Table 1). All FRAP measurements gave 100% fluorescence recovery (data not shown).

$D/D_0$  for FF in concentrated Ficoll solutions was always higher than  $(\eta/\eta_0)^{-1}$ , as we had noted previously for FF diffusing in concentrated protein solutions (Luby-Phelps et al., 1987).  $D/D_0$  for the smaller tracers deviated from  $(\eta/\eta_0)^{-1}$  more than for the larger tracers (see Discussion). Complete fluorescence recoveries were observed for all FRAP measurements (data not shown). The qualitative similarity of data for FF diffusing in concentrated Ficoll to FF diffusion in concentrated solutions of globular proteins (see also Luby-Phelps et al., 1987) suggests that the hydrodynamic properties of concentrated Ficoll solutions and concentrated protein solutions are very similar.

### Extent of actin polymerization in the presence of concentrated Ficoll or BSA

A sedimentation assay was used to test whether the extent of actin polymerization is altered in the presence of high concentrations of dissolved Ficoll or BSA. 1 ml of G-actin at 4 mg/ml was polymerized at room temperature in the presence and the absence of 7.7% F70. Both solutions were then centrifuged at 4°C at  $2 \times 10^5 g$  for 2 h.

TABLE 1  $D/D_0$  and  $\eta$  for Ficoll or BSA solutions

Concentration %	$\eta$ (measured) cP	$\langle D/D_0 \rangle$	$(\eta/\eta_0)^{-1}$
6.9 (Ficoll 400)	3.23	0.42	0.30
7.7 (Ficoll 400)	3.79	0.40	0.26
10.4 (Ficoll 70)	3.03	0.37	0.33
7.0 (BSA)	1.49	0.69	0.67

$D$ ,  $D_0$  are the diffusion coefficients of FF tracers in the matrix, buffer solutions, respectively. The  $\langle D/D_0 \rangle$  are the values for the largest tracers.  $\eta$ ,  $\eta_0$  are the bulk shear viscosities in the matrix, buffer solutions, respectively.

Determination of protein by the method of Bradford showed that both supernatants contained the same very low concentration of unsedimented protein:  $2.5 \pm 0.5 \mu\text{M}$ , or  $\sim 2.5\%$  of the starting concentration. Thus, within the limits of this test, Ficoll had no effect on the extent of G-actin polymerization and did not significantly reduce the average length of actin filaments. A similar test of the effect of 7% BSA on the extent of actin polymerization was more difficult to interpret. The concentration of protein in the supernatant was found to be approximately half that of a 7% BSA solution. This suggests that there may be some sort of association between BSA and F-actin leading to cosedimentation of the two proteins under our conditions. However, we note that BSA sediments appreciably under these conditions even in the absence of actin.

### Tracer diffusion in mixtures of F-actin with Ficoll or BSA

Fig. 3, *a-c*, shows  $D/D_0$  of FF in solutions of 3 mg/ml F-actin, 6.9% F400; 5 mg/ml F-actin, 10.4% F70; and 8 mg/ml F-actin, 7.7% F400, respectively. In all cases,  $D/D_0$  exhibited a size dependence similar to that observed in solutions of F-actin alone. However, the absolute

values of  $D/D_0$  for all tracers were reduced by inclusion of Ficolls. In fact, for each size fraction,  $D/D_0$  was reduced by a factor very close to the measured  $D/D_0$  for the same size fraction diffusing in the same concentration of Ficoll alone. This relationship can be expressed mathematically as  $D/D_{0(\text{Mixture})} = D/D_{0(\text{F-actin})} \times D/D_{0(\text{Ficoll})}$ . Comparison of the observed  $D/D_0$  with  $D/D_0$  predicted from this equation is shown in Fig. 3, *a-c*. As for tracer diffusing in F-actin alone or in Ficoll alone, all the FRAP data records for these experiments indicated 100% fluorescence recovery (data not shown). The fluorescence of the samples in these experiments was always spatially uniform, even for the largest tracer. This indicates that no phase separation between the filaments and the background Ficolls had taken place, because large tracer Ficolls would be expected to partition into the Ficoll phase resulting from phase separation.

Qualitatively similar results were obtained for FF diffusing in a mixture of 7 mg/ml F-actin, 7% BSA (Fig. 3 *d*).  $D/D_0$  in the mixture was within 30% of the value predicted by  $D/D_{0(\text{F-actin})} \times D/D_{0(\text{BSA})}$ , but the agreement was not as good as for F-actin and Ficoll mixtures, and the observed values of  $D/D_0$  were systematically greater than predicted by  $D/D_{0(\text{F-actin})} \times D/D_{0(\text{BSA})}$ .

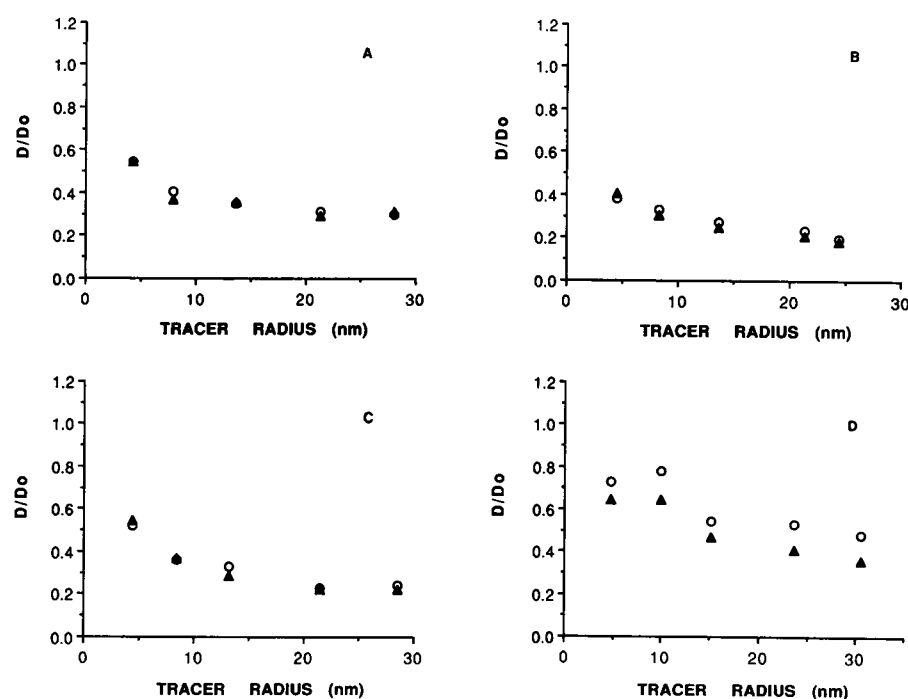


FIGURE 3 Observed  $D/D_0$  for FF in mixtures of F-actin and Ficoll (*A-C*) or BSA (*D*), compared with values predicted by  $D/D_{0(\text{F-actin})} \times D/D_{0(\text{Ficoll or BSA})}$ . (Open circles) Observed; (solid triangles) predicted. (*A*) 3 mg/ml F-actin, 6.9% F400. (*B*) 5 mg/ml F-actin, 10.4% F70. (*C*) 8 mg/ml F-actin, 7.7% F400. (*D*) 8 mg/ml F-actin, 7.0% BSA. In all F-actin and Ficoll mixtures, the observed data are closely approximated by the predicted values with a 6% average variance at each tracer radius. In F-actin and BSA mixtures, the observed data are systematically higher than predicted data with a deviation of  $\leq 30\%$ .

The discrepancy may reflect interaction between F-actin and BSA, as indicated by the simple sedimentation assay described above.

## DISCUSSION

The mean relative diffusion coefficient  $D/D_0$  of tracer particles in the cytoplasm of living cells is strongly dependent on the size of the tracer ( $R_H$ ) (Luby-Phelps et al., 1986, 1987), as if tracer diffusion is hindered by some sort of gel network. Linear extrapolation of the cellular data to  $R_H = 0$  gives  $D/D_0 \approx 0.3$ . Previous experiments have shown that this behavior cannot be accounted for simply by the high concentration of protein in cytoplasm (Luby-Phelps et al., 1986, 1987). The purpose of the experiments reported here was to see whether tracer diffusion in cytoplasm could be explained by either of two models: an entangled filament network in a dilute aqueous solvent, or an entangled filament network in a background solution of concentrated protein. F-Actin solutions were used as a model entangled filament network, and concentrated solutions of F70 or F400 were used to simulate concentrated solutions of cytoplasmic proteins. A further question, which is not addressed here, is whether cytoplasm is best represented by a cross-linked gel network, rather than an entangled filament network.

Tracer diffusion in solutions of F-actin alone was found to be size-dependent, in contrast to tracer diffusion in concentrated solutions of globular proteins or Ficoll particles (Fig. 1). Similar size dependence has recently been reported by Newman et al. (1989) for polystyrene spheres diffusing in F-actin solutions, although the polystyrene tracers were larger ( $25 < R_H < 250$  nm) and the F-actin concentrations lower than those used here. In both studies, the size dependence appeared much weaker than for FF diffusing in cytoplasm, and the linearly-extrapolated intercept at  $R_H = 0$  was  $\approx 1.0$ , rather than  $\approx 0.3$ . Because the concentrations of F-actin used in our experiments spanned the range of concentrations reported to occur in cytoplasm, these discrepancies suggest that cytoplasm cannot be solely an entangled actin network interpenetrated by a dilute fluid phase.

Tracer diffusion in mixtures of F-actin and high concentrations of Ficoll or BSA was also size-dependent and the linearly-extrapolated values of  $D/D_0$  at  $R_H = 0$  were substantially less than 1.0 (Fig. 3). In fact,  $D/D_0$  was well approximated by the product of  $D/D_0$  in F-actin alone and  $D/D_0$  in Ficoll or BSA alone. That is, for all five tracers used ( $3 < R_H < 32$  nm),

$$D/D_{0(\text{mixture})} = D/D_{0(\text{F-actin})} \times D/D_{0(\text{Ficoll or BSA})}. \quad (1)$$

Based on this result, both the existence of size-dependence and the fractional value of  $D/D_0$  obtained by linear extrapolation to  $R_H = 0$  for FF diffusing in cytoplasm might be explained by supposing that cytoplasm represents an entangled filament network interpenetrated by a crowded solution of globular proteins or other particles of size comparable to the tracer. To construct such a model, we first must discuss tracer diffusion in our reconstituted systems in terms of theories commonly applied to transport in porous media.

## Tracer diffusion in F-actin

The size dependence of FF diffusion in F-actin solutions can be attributed to the fact that the filaments in these solutions are highly entangled due to their extreme length and persistence length. At high ionic strength (e.g., 100 mM KCl, 2 mM  $\text{MgCl}_2$ ), G-actin polymerizes into long, filamentous, supramolecular polymers, referred to as F-actin filaments. At 1 mg/ml F-actin, there are 39  $\mu\text{m}$  of filament per cubic micrometer of solution. The average length of F-actin filaments at steady state has been estimated to be from 1 to 10  $\mu\text{m}$ , and their persistence length is also  $\geq 1$   $\mu\text{m}$  (Kawamura and Murayama, 1970; Tait and Frieden, 1982; Lanni and Ware, 1984; Janmey et al., 1986). However, because F-actin is susceptible to breakage under even the moderate shear stresses involved in handling, it is not clear how well these estimates reflect the average length of the undisturbed actin filaments arising from polymerization in our capillaries. In the absence of capping and severing proteins, only thermal motion is known to limit their length, and it is possible that the length of some filaments in pure actin solutions is determined solely by the dimensions of the container. Even non-gel-filtered actin, which contains at least one known capping protein (Cassela and Maack, 1987), has been estimated to have a weight average filament length of at least 2.2  $\mu\text{m}$  when polymerized at 1 mg/ml (Kawamura and Murayama, 1970). The length distribution of the population of filaments is even less well characterized than the average length, although it is in principle exponential at steady state (Oosawa, 1970).

Based on the available estimates of the length and persistence length of F-actin, our solutions of F-actin are entangled by the accepted definition. According to Doi and Edwards (1986), a solution of rigid, rodlike polymers falls into one of three concentration domains defined by the parameters,  $c_1 = 1/L^3$  and  $c_2 = 1/bL^2$ , where  $b$  and  $L$  are the diameter and the length of the rods, respectively. In dilute solutions, the polymer (rod) number concentration,  $c$ , satisfies  $c \leq c_1$ . In semidilute solutions,  $c_1 \leq c \leq c_2$ , and in concentrated solutions  $c \geq c_2$ . In the semidilute domain, the lateral movement of the polymers is severely restricted by "entanglement" among filaments (rods). In the concen-

trated domain, longitudinal movement is restricted as well as lateral movement, and spontaneous, nematic ordering of the polymers may take place. Taking the values  $L = 5 \times 10^{-4}$  cm,  $b = 10 \times 10^{-7}$  cm for F-actin filaments,  $c_1 = 8 \times 10^9$  filaments per milliliter. This corresponds to an actin weight concentration of  $\sim 1$   $\mu$ g/ml. Thus, all the concentrations used in our experiments were well into the entanglement regime. At 1 mg/ml, which is the lowest concentration used in these experiments, filaments enter the entanglement regime when  $L$  becomes 161 nm, or about 60 monomers long. In fact, for  $L$  and  $b$  as above, all the concentrations used are in the concentrated solution regime because  $c_2 = 4.0 \times 10^{13}$  per milliliter (a weight concentration of  $\approx 1$  mg/ml). However, at even the highest F-actin concentration used (12 mg/ml), no filament alignment was observed in our samples by differential interference contrast microscopy or polarization microscopy, suggesting that no large-scale phase separations due to local ordering had occurred. The absence of an immobile fraction in any of our measurements also suggests that tracer was not trapped or partitioned into any portion of the matrix, either due to phase separation, or due to the mesh size of the entangled network.

Due to entanglement, as well as the length of F-actin filaments at these concentrations, their translational diffusion is negligible ( $D \ll 10^{-9}$  cm<sup>2</sup>/s) (Lanni and Ware, 1984; Simon et al., 1988a; Tait and Frieden, 1982) compared with the diffusion of tracers ( $D > 10^{-8}$  cm<sup>2</sup>/s). Thus, to a compact tracer particle, entangled F-actin solutions can be considered as a system consisting of two phases: a filament network phase, from which the tracer is excluded; and a fluid phase, in which the tracers diffuse. The filaments may affect tracer diffusion in two ways. One is an excluded volume, or "obstruction" effect, where the possible diffusion paths of the tracer are eliminated in the volume occupied by the network phase. The other is a hydrodynamic effect, where the average hydrodynamic friction on the tracer is increased due to interactions of the fluid phase with the filaments of the network phase. The latter is similar to a wall effect (Happel and Brenner, 1973), where the effective friction on a tracer diffusing close to a solid wall (or diffusing through a cylinder) increases sharply as the distance between the tracer and the wall becomes comparable to the tracer radius.

Most theoretical treatments of tracer diffusion or mobility in gels, colloidal suspensions, or porous media have been limited to either the excluded-volume effect (Fricke, 1924; Wang, 1954; Lauffer, 1961; Ogston et al., 1973) or the hydrodynamic effect (Brinkman, 1947; Batchelor, 1972; Howells, 1974; Cukier, 1983, 1984; Altenberger and Tirrell, 1984; Phillies, 1989). Both the excluded volume models and the hydrodynamic models predict that  $D/D_0$  decreases with increasing  $R_H$ , but with

a different dependence on matrix concentration (or matrix volume fraction):

$$(D/D_0)_{\text{excl. vol.}} = 1 - \alpha \phi_0 + \dots \quad (2)$$

$$(D/D_0)_{\text{hydro.}} = 1 - \beta \phi_0^{1/2} + \dots, \quad (3)$$

where  $\phi_0$  is the volume fraction of matrix material,  $\alpha$  is a coefficient defined in the limit of very small tracer particles ( $R_H \rightarrow 0$ ), and  $\beta$  is a function of  $R_H$  that equals zero for  $R_H \rightarrow 0$ . An exception to this generalization is the obstruction model of Ogston et al. (1973), which predicts a square-root dependence on matrix concentration, as in the hydrodynamic models:

$$D/D_0 = \exp [ - (\pi \lambda)^{1/2} R_H ], \quad (4)$$

where  $\lambda$  is the length density (micrometer filament/micrometer<sup>3</sup>). However, this model is in disagreement with a large body of results on transport in composite media that show first-order dependence on  $\phi_0$  (or  $\lambda$ ), as in Eq. 2. This may be because the model of Ogston et al. is based on a picture of tracer-matrix interactions in which steps are completely eliminated from the diffusion path when the tracer is in close proximity to the matrix obstructions. As we have pointed out previously (Luby-Phelps et al., 1988), this may be equivalent to introducing solvent-mediated hydrodynamics as a severe but very short-range interaction.

The specific case of the hydrodynamic effect on a diffusing spherical particle in a random matrix of rodlike macromolecules was treated in a condensed form by Cukier (1984) with the result:

$$D/D_0 = \exp ( - \kappa R_H ), \quad (5)$$

Where  $R_H$  is the radius of the tracer particle, and  $\kappa$  is a matrix-dependent hydrodynamic screening constant. The important characteristic of  $\kappa$  is that in sparse matrices, it is proportional to the square root of the volume fraction ( $\phi_0$ ) or length density ( $\lambda$ ) of fixed matrix particles, as in Eq. 3.

For each data set,  $D/D_0 = f(R_H)$ , corresponding to the five F-actin concentrations used, we estimated  $\kappa$  via a weighted least-squares fit of Eq. 5 (Table 2). As shown in Fig. 4,  $\kappa$  was found to vary approximately as the 0.67 power of  $\lambda$ , close to the hydrodynamic limit of 0.50. The best-fit exponential curves fall within 15% error for each data set. The curve for 12 mg/ml actin data is shown in Fig. 5 as an example. We conclude that for the actin concentration range tested, FF diffusion is dominated by the hydrodynamic interaction between tracer and filaments, the direct obstruction effect being secondary.

The hydrodynamic screening constant ( $\kappa$ ) can also be expressed in terms of the length ( $L$ ), diameter ( $b$ ), and length density ( $\lambda$ ) of rodlike matrix polymers;  $\kappa =$

TABLE 2 Values of  $\kappa$  and  $L^*$  for FF diffusing in F-actin

Actin concentration	$\kappa$	$L_{\text{eff}}$
mg/ml	$\mu\text{m}^{-1}$	$\mu\text{m}$
1.0 (39) <sup>‡</sup>	6.8	30.0
3.0 (117)	15.3	1.08
5.0 (195)	23.6	0.27
8.0 (312)	27.2	0.54
12.0 (468)	36.7	0.32

\*Weighted least-squares fit to the hydrodynamic theory of Cukier (1984). See text, Eq. 5.

<sup>‡</sup>Values in parentheses are filament length density ( $\lambda$ ) in units of micrometers filament per cubic micrometer.

$[3\pi\lambda/\ln(L/b)]^{1/2}$ . Using  $b = 10$  nm for F-actin (Egelman and Padron, 1984), and the least-squares estimates of  $\kappa$ , we calculated the effective hydrodynamic length ( $L_{\text{eff}}$ ) of actin filaments at each actin concentration. As shown in Table 2,  $L_{\text{eff}}$  is much shorter than the estimated length of actin filaments ( $\approx 10$   $\mu\text{m}$ ) except at 1 mg/ml. Because of hydrodynamic screening by the relatively immobile filaments, we expect that  $L_{\text{eff}}$  will be a decreasing function of filament number density. Values of  $L_{\text{eff}}$  in Table 2 are generally consistent with this hypothesis, but show too much variance for mathematical analysis.

One of the simplifications that is made to obtain a tractable hydrodynamic model is that the matrix polymers are fixed in the system. To a certain extent, this assumption is realistic for F-actin solutions, because the diffusion coefficient of FF ( $> 10^{-8}$   $\text{cm}^2/\text{s}$ ) is much greater than the diffusion coefficient of the F-actin filaments ( $< 10^{-9}$   $\text{cm}^2/\text{s}$ ) (Lanni and Ware, 1984; Tait and Frieden, 1982). However, the possibility of low-amplitude segmental motion of the filaments (filament flexibility) is not considered in these models. An alternative treatment, which exchanges the fixed obstruction assumption for a

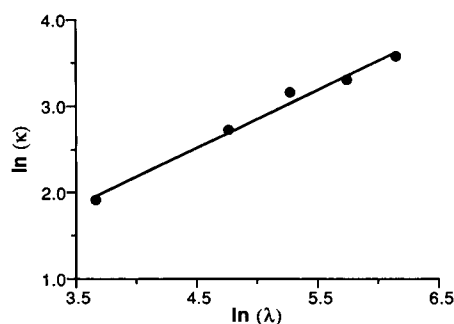


FIGURE 4 Graph of the logarithm of the exponential screening constant ( $\kappa$ ,  $\mu\text{m}^{-1}$ ) versus the logarithm of the F-actin filament density ( $\lambda$ ,  $\mu\text{m}$  filament/ $\mu\text{m}^3$ ).  $\kappa$  was the weighted least-squares estimate for each actin data set (1, 3, 5, 8, and 12 mg/ml). The solid line is the least-squares power-law relation  $\kappa = (0.62)(\lambda)^{0.67}$ .

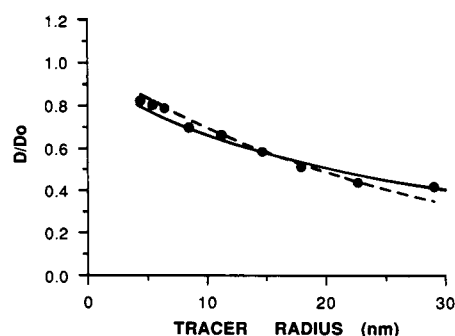


FIGURE 5 Comparison of measured  $D/D_0$  for FF diffusing in 12 mg/ml F-actin (data points) to curves predicted by the hydrodynamic theories of Cukier (dashed curve) and of Phillies (solid curve). Cukier (1984) predicts  $D/D_0 = \exp(-\kappa R_H)$ . The best-fitting values of  $\kappa$  for each concentration of F-actin gave values of  $D/D_0$  within 15% of actual  $D/D_0$ . Phillies (1989) predicts  $D/D_0 = \exp(-\alpha c' R_H^\nu)$ . A weighted least-squares fit to the combined data sets for all concentrations of F-actin gave  $\alpha = 0.021$ ,  $\nu = 0.53$ , and  $\delta = 0.72$ . For each concentration of F-actin, this equation fits actual  $D/D_0$  with an error of  $\leq 10\%$ .

self-similarity assumption, has been developed by Phillies (1989). This results in a universal relation for  $D/D_0$  for a solution or melt of mobile or flexible polymers:

$$D/D_0 = \exp(-\alpha c' R_H^\delta), \quad (6)$$

where  $c$  is the concentration of filaments (proportional to  $\phi$  or  $\lambda$ ), and  $\alpha$ ,  $\nu$ , and  $\delta$  are constants. Using a weighted least-squares minimization (de Levie, 1986) to determine the constants  $\alpha$ ,  $\nu$ , and  $\delta$  for our aggregate data set,  $D/D_0 = f(R_H, c)$  of 38 data points, we find

$$D/D_0 = \exp(-0.021 c^{0.53} R_H^{0.72}) \quad (7)$$

for FF diffusing in F-actin solutions, where  $c$  is in milligrams per milliliter and  $R_H$  is in nanometers. The above function is compared with data for 12 mg/ml F-actin in Fig. 5. The nearly square-root dependence on matrix concentration again indicates that, at least at low F-actin volume fraction ( $\phi_0 \approx 0.037$  at 12 mg/ml), direct excluded volume or obstruction effects are small, and our data can be explained in terms of hydrodynamic interactions between the tracer and the matrix.

In principle, the dependence of  $D/D_0$  on  $c$  and  $R_H$  should be described by one set of parameters over a wide range of tracer sizes and F-actin concentrations. However, Newman et al. (1989) obtained quite a different value for  $\nu$  ( $=1.08$ ) for their data, although the dependence on  $R_H$  was very similar to ours ( $\delta = 0.73$ ). This discrepancy might reflect unexpected interactions of polystyrene spheres with actin filaments due to their surface charges, although Newman et al. argue against this. Another difference is in the method used to measure



diffusion. Quasielastic light scattering, used by Newman et al., generally is sensitive to local diffusion, whereas FRAP measures only long-range diffusion. More interesting is the possibility that because the size range of polystyrene spheres is significantly larger than for FF, the direct obstruction effect is much more significant in the experiments of Newman et al., leading to an approximate first-order dependence on actin concentration, as in Eq. 2.

An assumption that has been made thus far in our discussion is that FF do not bind to F-actin filaments. Slow-exchange interactions are ruled out by the absence of an immobile fraction and by the fact that the diffusion coefficients of FF are at least two orders of magnitude higher than the diffusion coefficients of F-actin (see Results). Although at present we cannot absolutely rule out the possibility that the size dependence of FF diffusion in the presence of F-actin reflects size-dependent, transient binding, there are several arguments against this. First, because FF have a very low density of ionizable residues and are quite hydrophilic, it is unlikely that they will form charge or hydrophobic interactions with F-actin or other proteins. Second, the size dependence is correctly estimated by hydrodynamic theory (Cukier, 1984) with no adjustable parameters. Third, there is no apparent mass action effect on the diffusion coefficient of FF in the presence of F-actin when a high concentration of unlabeled Ficoll is included in the solution: If the diffusion coefficients we measured for FF in the presence of F-actin are in fact a function of the exchange rate of a transient complex of tracer and F-actin, the addition of large amounts of Ficoll should reduce the interaction of the tracer Ficolls with F-actin, increasing the measured diffusion coefficient for a given tracer. Instead, when the increased viscosity due to the excess Ficoll is corrected for, we obtain exactly the diffusion coefficient for the same size tracer in F-actin alone. This is expressed in the product relationship we described in Results (Eq. 1).

### Tracer diffusion in concentrated Ficoll solutions

In solutions of Ficoll or globular proteins, where the background particles are mobile, we always observed  $D/D_0 > (\eta/\eta_0)^{-1}$ , with  $D/D_0$  for small particles somewhat greater than  $D/D_0$  for large particles (Fig. 2), although this size dependence was very weak. This may be explained by considering the relative sizes of the tracer and background solute particles. To a tracer much larger than the background solute particles, the background solution will appear to be a continuum (Mondy et al., 1986), and the problem is simply reduced to the diffusion of a tracer in a Newtonian fluid, where  $D/D_0 = (\eta/\eta_0)^{-1}$ . A well-recognized example of this is the diffusion of tracers in water or other simple solvents, where the size of

the solvent molecules is negligible compared with those of the tracers. At the other extreme, when the size of the tracer is much smaller than that of the background solute particles, the root mean square displacement of the tracers in any time interval will be much larger than that of the background particles, and the background particles can be approximated as stationary obstacles. Thus, the tracer can be regarded as diffusing in the void volume of a gel, and  $D/D_0$  will be closer to the pure obstruction effect value, which we expect to be significantly higher than  $(\eta/\eta_0)^{-1}$ .

The diffusion of FF in solutions of Ficoll or globular proteins falls between these two extremes. Because no sudden transition is expected in such well-defined systems,  $D/D_0$  shows weak size dependence as seen in Fig. 2, approaching  $(\eta/\eta_0)^{-1}$  for large tracers (see also Luby-Phelps et al., 1987). According to this view,  $D/D_0$  more closely approximates  $(\eta/\eta_0)^{-1}$  in F70 than in F400 because the background particles are smaller relative to the tracer (see Table 1). FF diffusion in concentrated solutions of BSA shows less size dependence than in concentrated solutions of unfractionated Ficoll because the BSA molecules are comparable in size to the smaller tracer particles, whereas unfractionated Ficoll contains a wide range of particle sizes, including many that are considerably larger than the tracer particles (see Appendix).

For the purpose of modeling tracer diffusion in cytoplasm, we fit the data for diffusion of FF in Ficoll solutions to the universal scaling equation (Eq. 6), and obtained the following relation:

$$D/D_0 = \exp(-0.035 c^{0.635} R_H^{0.16}). \quad (8)$$

It is interesting to note that the prefactor,  $\alpha$ , and the concentration dependence,  $\nu$ , are very similar to the values for FF diffusing in F-actin, while the size-dependence is much weaker. In fact, the size dependence is very close to the value of  $0 \pm 0.2$  predicted in Phillies' universal scaling theory (Phillies, 1989). The stronger size dependence in F-actin solutions may reflect the extreme length and large persistence length of the filaments.

One way in which Ficolls are not good models for globular proteins is that they are not so compact and may be able to interpenetrate on another. In crowded solutions, interpenetration may become significant, perhaps changing the hydrodynamic behavior of the particles. The probability of interpenetration becomes 1.0 at the volume fraction ( $\phi^*$ ) where close packing of the particles occurs. For hexagonal close-packing of spheres,  $\phi^*$  is 0.74. For random close-packing,  $\phi^*$  will be 85% of this value or 0.63 (Chandler et al., 1983). At the highest concentration of F400 we used in our experiments (7.7%), the number average volume fraction was 0.56 (see Appendix). Thus,

although our Ficoll solutions are very crowded, on the average they are not close packed, and interpenetration should not be a major factor in the hydrodynamics of the system.

## Tracer diffusion in F-actin and Ficoll mixtures

In a mixture of long filaments and compact background particles, the effect of the F-actin filaments on FF diffusion should not be any different from that in an F-actin solution alone, because we do not expect any changes in the physical shape and distributions of F-actin filaments in the presence of Ficoll solutions. Although the presence of Ficoll at high concentrations appeared to have little effect on the extent of actin polymerization (see Results), the effect of Ficoll on the length distribution of F-actin filaments is not known. However, because the effect of F-actin on diffusion of FF results from the immobility of the filaments, as long as the F-actin filaments are entangled, slight changes in F-actin length distribution should not affect the results obtained in this study. This idea is supported by our observation that FF diffusion in gel-filtered actin was not significantly different from FF diffusion in SW actin, although the average length of filaments formed from gel-filtered actin is thought to be much longer (Tait and Frieden, 1982; Pollard and Cooper, 1986). Calculated according to Doi and Edwards (1986), the average filament length needed for entanglement at the lowest concentration of F-actin in our mixtures of F-actin and Ficoll (3 mg/ml) is ~93 nm, which is ~34 actin monomers. Because the actin concentrations were many times greater than the critical concentration for polymerization, because of the large increase of viscosity observed upon adding KCl and  $MgCl_2$ , and because our sedimentation assay did not indicate an increase in nonsedimentable filaments in the supernatant, it seems certain that the filaments in the mixtures of F-actin and Ficoll are long enough to be entangled.

The hydrodynamic interaction with the background particles in the fluid phase is more complicated. In the presence of F-actin filaments, the hydrodynamic properties of the Ficoll particles close to F-actin filaments will be subject to wall effects, which increase the hydrodynamic friction in the fluid phase compared with Ficoll solutions of the same concentration in the absence of F-actin filaments. This, in effect, increases the apparent viscosity of the background fluid near the filaments. But provided that the filament volume fraction ( $\phi_0$ ) is low enough, and interfilament spacing is much greater than the size of the background particles, this effect can be neglected. Even though 8 mg/ml F-actin is a concentrated solution by biochemical standards,  $\phi_0$  is very low (0.025). Therefore, our mixtures can be thought of as an F-actin solution in

which the reference phase is a Ficoll solution rather than an aqueous buffer solution. Thus,

$$D_{(\text{mixture})}/D_{(\text{Ficoll})} = D_{(\text{F-actin})}/D_{(\text{water})}. \quad (9)$$

By substitution, this becomes  $D/D_{O(\text{mixture})} = D/D_{O(\text{F-actin})} \times D/D_{O(\text{Ficoll})}$  (Eq. 1), as we have observed.

## Modeling cytoplasm

The relationship expressed in Eq. 1 can be used to model cytoplasm as a three-component system, having a network phase consisting of cytoskeletal filaments, and a fluid phase composed of solvent (water) with a high concentration of globular proteins or other macromolecules. Using values of  $\alpha$ ,  $\nu$ , and  $\delta$  obtained from the study of FF diffusion in F-actin (Eq. 7),  $D/D_{O(\text{filaments})} = \exp(-0.021 c_f^{0.53} R_H^{0.72})$  where  $c_f$  is the concentration of filaments in milligrams per milliliter. Similarly, from Eq. 8,  $D/D_{O(\text{particles})} = \exp(-0.035 c_p^{0.635} R_H^{0.16})$  where  $c_p$  is the concentration of background particles in milligrams per milliliter. Since, from Eq. 1,  $D/D_{O(\text{cytoplasm})} = D/D_{O(\text{filaments})} \times D/D_{O(\text{particles})}$ , we fitted our cytoplasmic data (Luby-Phelps et al., 1987) by weighted least squares to the equation  $D/D_O = \exp(-0.021 c_f^{0.53} R_H^{0.72}) \times \exp(-0.035 c_p^{0.635} R_H^{0.16})$ , treating  $c_f$  and  $c_p$  as undetermined parameters. This gave  $c_f = 37$  mg/ml and  $c_p = 124$  mg/ml, or 12.4%. Calculated from a value of 10 nm for the diameter of an F-actin filament, this concentration of filaments corresponds to an excluded volume fraction of ~0.11. The estimated filament concentration is 5–10 times higher than the reported concentrations of actin or other cytoskeletal filament proteins (Bray and Thomas, 1975; Hiller and Weber, 1978; Nagle et al., 1977; Blikstad et al., 1978). However, the model does not require that the filament system be composed of F-actin. Any entangled filament system occupying the same volume fraction will produce the same effect. In this context, it is interesting to note that the volume fraction estimated from our model (0.11) is close to, but somewhat less than the volume fraction occupied by the microtrabecular lattice (0.16) as determined morphometrically from high voltage electron micrographs (Gershon et al., 1985).

Comparison of the cytoplasmic data with values predicted by the fitted function is shown in Fig. 6. The agreement is within 10% for all sizes of tracer except the two largest, where the fitted function overestimates the actual  $D/D_O$  by nearly 100%. These are also the sizes of tracer where an immobile fraction appears in some FRAP records for FF diffusing in cytoplasm (Luby-Phelps et al., 1987). Fluorescence ratio imaging has shown that large tracer particles are excluded from some domains of the cytoplasmic volume, as if the cytomatrix in these domains had a percolation cutoff radius in the neighborhood of 25 nm (Luby-Phelps and Taylor, 1988). Because the values

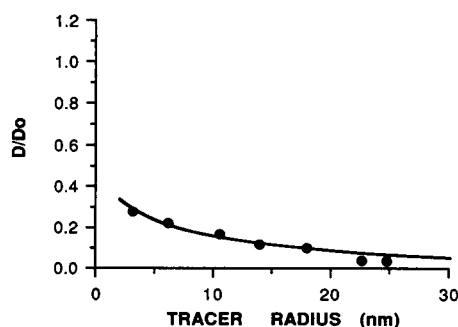


FIGURE 6 Comparison of  $D/D_0$  in cytoplasm (data points) with the  $D/D_0$  predicted by  $D/D_0 = \exp(-0.021 c_i^{0.53} R_{Hi}^{0.72}) \times \exp(-0.035 c_p^{0.635} R_{Hi}^{1.6})$  (fitted curve). The standard deviations of the fitted curve from the measured result are within 10% except for the two largest tracer size fractions. Data taken from Luby-Phelps et al., 1987.

of  $D$  in cytoplasm were averaged without regard to the subcellular location of each measurement, it is possible that the difference between observed and predicted  $D/D_0$  for the largest tracers reflects a percolation cutoff due to cross-linking of the filament network in at least some domains of the cytoplasm. We are currently testing this hypothesis by studying the diffusion of FF in gels of F-actin that is noncovalently cross-linked with actin-binding proteins.

## APPENDIX

### Estimation of Ficoll molecular size parameters

Measurements of the tracer diffusion coefficient for Ficoll fractions that were selected to span the size-exclusion chromatogram provide our most detailed estimate of molecular size. For each fraction, the amount of fluorescein dye bound to the polymer was measured by optical absorbance at 495 nm, total carbohydrate was measured by an anthrone assay, and the average hydrodynamic radius ( $R_{Hi}$ ) was calculated from the aqueous diffusion coefficient measured by FRAP. From these three parameters, we found that the absorbance (or fluorescence) of the labeled polymer scales approximately as the 2.5 power of  $R_{Hi}$ :

$$F_i = a_F c_i R_{Hi}^{2.5},$$

where  $c_i$  is the number density of Ficoll molecules (in molecules per milliliter) of size  $R_{Hi}$ , and  $a_F$  is an undetermined constant. An exponent of 2.0 is expected for surface labeling and 3.0 for volume labeling of spherical molecules. The observed value, 2.5, most likely reflects a fractal character to the branched structure of Ficoll polymers.

Defining the concentration scale:

$$c'_i = \frac{F_i}{R_{Hi}^{2.5}} = a_F c_i.$$

$a_F$  can be defined in terms of  $\{c'_i\}$  and  $\{c_i\}$ :

$$a_F = \frac{\sum c'_i}{\sum c_i}.$$

If the number-average molecular weight ( $M_n$ ) for the unfractionated Ficoll is known,  $\sum c_i$  can be replaced by known quantities:

$$M_n = \frac{\sum c_i M_i}{\sum c_i} = N_{AV} \frac{\sum c_i m_i}{\sum c_i}$$

and

$$c_p = \sum c_i m_i = \frac{M_n}{N_{AV}} \sum c_i,$$

where  $c_p$  is the total polymer concentration in grams per milliliter. Therefore,

$$a_F = \frac{\sum c'_i}{\frac{M_n}{N_{AV}} \sum c_i}.$$

The volume fraction ( $\phi$ ) occupied by the hydrodynamically-effective Ficoll molecules is simply the sum over all sizes of the concentration-weighted molecular volume ( $V_i$ ):

$$\begin{aligned} \phi &= \sum c_i V_i = \frac{4}{3} \pi \sum c_i R_{Hi}^3 = \frac{4}{3} \pi \sum \frac{c'_i}{a_F} R_{Hi}^3 \\ &= \frac{c_p}{M_n} N_{AV} \frac{4}{3} \pi \frac{\sum c'_i R_{Hi}^3}{\sum c'_i} = \frac{c_p}{M_n} N_{AV} \frac{4}{3} \pi \frac{\sum F_i R_{Hi}^{0.5}}{\sum F_i R_{Hi}^{-2.5}}. \end{aligned}$$

Therefore, the volume fraction occupied by Ficoll molecules can be estimated from  $M_n$ ,  $c_p$ , and the number average of  $R_{Hi}^3$ . The latter can be calculated from the combined chromatographic and FRAP data. For F400, a value of  $M_n = 169$  kD can be derived from osmotic pressure data (Pharmacia Product Information). Using values of  $F_i$  and  $R_{Hi}$  for nine fractions that span the chromatogram, we estimate

$$\left( \frac{\sum c'_i R_{Hi}^3}{\sum c'_i} \right)^{1/3} = (R_{Hi}^3)_n^{1/3} = 7.87 \text{ nm},$$

and for  $c_p = 7.7\% = 0.077$  g/ml,  $\phi = 0.56$ .

The above estimate of average size is close to that derived from  $M_n$  and the intrinsic viscosity of F400, 7.7 nm, but is significantly less than the size derived from osmotic pressure data, 10.6 nm. We note that  $\phi = 0.56$  is close to the volume fraction corresponding to "random close packing" of monodisperse spheres (see text), but expect that because unfractionated Ficoll is quite polydisperse, a 7.7% solution is not actually as close to this limit.

We thank Chrisanth Thompson, Judy Montibeller and Del McCaslin for their technical assistance. We thank Dr. D. Lansing Taylor for his critical review and encouragement of this project at several stages.

This research was supported by National Science Foundation grant DCB86-16089 (K. Luby-Phelps), National Institutes of Health grant GM 34639 (F. Lanni), and NIH grant AR 32461 (D. L. Taylor).

*Received for publication 20 October 1989 and in final form 21 February 1990.*

*Note added in proof:* To rule out transient binding between FF and F-actin, we measured the equilibration of FF ( $R_H = 8.5$  nm) between a buffer phase and an F-actin phase separated by a filter membrane (8- $\mu$ m pore size, type SC, Millipore Corp.). The final fluorescence level (arbitrary units) was  $6.25 \pm 0.25$  on the buffer side of the membrane and  $5.75 \pm 0.25$  on the actin side, regardless of whether FF was introduced with the buffer or with the actin. (A slightly lower value on the actin side is expected due to the excluded volume of the actin filaments.) A

Bradford protein assay showed that F-actin remained assembled and did not cross the membrane during the experiment. These results confirm that the interactions between FF and F-actin are primarily hydrodynamic and that binding interactions are negligible.

## REFERENCES

- Allen, R. D. 1961. Ameboid movement. In *The Cell*. Vol. 2. J. Brachet, editor. Academic Press, Inc. New York. 135–216.
- Altenberger, A. R., and M. Tirrell. 1984. On the theory of self-diffusion in a polymer gel. *J. Chem. Phys.* 80:2208–2213.
- Anderson, N. G., and J. G. Green. 1967. The soluble phase of the cell. In *Enzyme Cytology*. D. B. Roodyn, editor. Academic Press, Inc., New York. 475.
- Batchelor, G. K. 1972. Sedimentation in a dilute suspension of spheres. *J. Fluid Mech.* 52:245.
- Blikstad, I., F. Markey, L. Carlsson, T. Persson, and U. Lindberg. 1978. Selective assay of monomeric and filamentous actin in cell extracts using inhibition of deoxyribonuclease I. *Cell*. 15:935–943.
- Bray, D., and C. Thomas. 1975. The actin content of fibroblasts. *Biochem. J.* 147:221–228.
- Brinkman, H. C. 1947. A calculation of the viscous force exerted by a flowing fluid on a dense swarm of particles. *Appl. Sci. Res.* A1:27.
- Cassela, J. F., and D. J. Maack. 1987. Cap Z(36/32) is a contaminant and the major inhibitor of actin network formation in conventional actin preparations. *Biochem. Biophys. Res. Commun.* 145:625–630.
- Chandler, D., J. D. Weeks, and H. C. Andersen. 1983. Van der Waals picture of liquids, solids, and phase transformations. *Science (Wash. DC)*. 220:787–794.
- Clegg, J. S. 1984. Properties and metabolism of the aqueous cytoplasm and its boundaries. *Am J. Physiol.* 246:R133–R151.
- Conklin, E. G., 1940. Cell and protoplasm concepts: historical account. In *The Cell and Protoplasm*. F. R. Mouton, editor. Science Press, Lancaster, PA. 6–19.
- Cukier, R. I. 1983. Diffusion of interacting Brownian particles in a fluid with fixed macroparticles. *J. Chem. Phys.* 79:3911–3920.
- Cukier, R. I. 1984. Diffusion of Brownian spheres in semidilute polymer solutions. *Macromolecules*. 17:252–255.
- Deen, W. M., M. P. Bohrer, and N. B. Epstein. 1981. Effects of molecular size and configuration on diffusion in microporous membranes. *AIChE (Am. Inst. Chem. Eng.) J.* 27:952–959.
- de Levie, R. 1986. When, why, and how to use weighted least squares. *J. Chem. Ed.* 63:10–15.
- De Robertis, E. D. P., W. W. Nowinski, and F. A. Saez. 1970. *Cell Biology*. W. B. Saunders Co., Philadelphia, PA. 47.
- Doi, M., and S. F. Edwards. 1986. *The Theory of Polymer Dynamics*. Clarendon Press, Oxford, UK. 324–378.
- Engelman, E. H., and R. Padron. 1984. X-Ray diffraction evidence that actin is a 100 Å filament. *Nature (Lond.)*. 307:56–58.
- Elson, E. L., and H. Qian. 1989. Interpretation of fluorescence correlation spectroscopy and photobleaching recovery in terms of molecular interactions. *Methods Cell Biol.* 30:307–332.
- Frey-Wyssling, A. 1953. *Submicroscopic Morphology of Protoplasm*. Elsevier Science Publishing Co., New York. 411.
- Fricke, H. 1924. A mathematical treatment of the electric conductivity and capacity of disperse systems. *Physiol. Rev.* 24:575–587.
- Fulton, A. B. 1982. How crowded is the cytoplasm? *Cell*. 30:345–347.
- Gershon, N. D., K. R. Porter, and B. L. Trus. 1985. The cytoplasmic matrix: its volume and surface area and the diffusion of molecules through it. *Proc. Natl. Acad. Sci. USA*. 82:5030–5034.
- Happel, J., and H. Brenner. 1973. *Low Reynolds Number Hydrodynamics: With Special Applications to Particulate Media*. Noordhoff International Publishing, Leyden, The Netherlands. 286–357.
- Hartwig, J. H., and T. P. Stossel. 1979. Cytochalasin B and the structure of actin gels. *J. Mol. Biol.* 134:539–553.
- Hiller, G., and K. Weber. 1978. Radioimmunoassay for tubulin: a quantitative comparison on the tubulin content of different established tissue culture cells and tissues. *Cell*. 14:795–804.
- Houk, T. W., and K. Ue. 1974. The measurement of actin concentration in solution: a comparison of methods. *Anal. Biochem.* 62:66–74.
- Howells, I. D. 1974. Drag due to the motion of a Newtonian fluid through a sparse random array of small fixed rigid objects. *J. Fluid Mech.* 64:449–475.
- Janmey, P. A., J. Peetermans, K. S. Zaner, T. P. Stossel, and T. Tanaka. 1986. Structure and mobility of actin filaments as measured by quasioelectric light scattering, viscometry and electron microscopy. *J. Biol. Chem.* 261:8357–8362.
- Kawamura, M., and K. Murayama. 1970. Electron microscopic particle length of F-actin polymerized in vitro. *J. Biochem.* 67:437–457.
- Lanni, F., and B. R. Ware. 1984. Detection and characterization of actin monomers, oligomers, and filaments in solution by measurement of fluorescence photobleaching recovery. *Biophys. J.* 46:97–110.
- Lanni, F., A. S. Waggoner, and D. L. Taylor. 1985. Structural organization of interphase 3T3 fibroblasts studied by total internal reflection fluorescence microscopy. *J. Cell. Biol.* 100:1091–1102.
- Lardy, H. A. 1965. On the direction of pyridine nucleotide oxidation-reduction reactions in gluconeogenesis and lipogenesis. In *Control of Energy Metabolism*. B. Chance, R. Estabrook, and J. R. Williamson, editors. Academic Press, Inc., New York. 246.
- Lauffer, M. A., 1961. Theory of diffusion in gels. *Biophys. J.* 1:205–213.
- Laurent, T. C. 1967. Determination of the structure of agarose gels by gel chromatography. *Biochim. Biophys. Acta*. 136:199–205.
- Laurent, T. C., and K. A. Granath. 1967. Fractionation of dextran and Ficoll by chromatography on Sephadex G-200. *Biochim. Biophys. Acta*. 136:191–198.
- Luby-Phelps, K. 1989. Preparation of fluorescently labeled dextrans and ficolls. *Methods Cell Biol.* 29:59–73.
- Luby-Phelps, K., and D. L. Taylor. 1988. Subcellular compartmentalization by local differentiation of cytoplasmic structure. *Cell Motil.* 10:28–37.
- Luby-Phelps, K., D. L. Taylor, and F. Lanni. 1986. Probing the structure of cytoplasm. *J. Cell. Biol.* 102:2015–2022.
- Luby-Phelps, K., P. E. Castle, D. L. Taylor, and F. Lanni. 1987. Hindered diffusion of inert tracer particles in the cytoplasm of mouse 3T3 cells. *Proc. Natl. Acad. Sci. USA*. 84:4910–4913.
- Luby-Phelps, K., F. Lanni, and D. L. Taylor. 1988. The submicroscopic properties of cytoplasm as a determinant of cellular function. *Annu. Rev. Biophys. Biophys. Chem.* 17:369–396.
- Marsland, D. A. 1942. Protoplasmic streaming in relation to gel structure in the cytoplasm. In *The Structure of Protoplasm: A Monograph of the American Society of Plant Physiologists*. W. Seifriz, editor. Iowa State College Press, Ames, IA. 127.
- Mondy, L. A., A. L. Graham, and J. L. Jensen. 1986. Continuum approximations and particle interactions in concentrated suspensions. *J. Rheol.* 30:1031–1051.
- Nagle, B. W., K. H. Doenges, and J. Bryan. 1977. Assembly of tubulin from cultured cells and comparison with the neurotubulin model. *Cell*. 12:573–586.

- Newman, J., N. Mroczka, and K. L. Schick. 1989. Dynamic light scattering measurements of the diffusion of probes in filamentous actin solutions. *Biopolymers*. 28:655-666.
- Ogston, A. G., B. N. Preston, and J. D. Wells. 1973. On the transport of compact particles through solutions of chain-polymers. *Proc. R. Soc. Lond. A*. 333:297-316.
- Oosawa, F. 1970. Size distribution of protein polymers. *J. Theor. Biol.* 27:69-86.
- Phillies, G. D. J. 1987. Dynamics of polymers in concentrated solutions: the universal scaling equation derived. *Macromolecules*. 20:558-564.
- Phillies, G. D. J. 1989. The hydrodynamic scaling model for polymer self-diffusion. *J. Phys. Chem.* 93:5029-5039.
- Pollard, T. D. 1984. Molecular architecture of the cytoplasmic matrix. In *White Cell Mechanics: Basic Science and Clinical Aspects*. Alan R. Liss, Inc., New York. 75-86.
- Pollard, T. D., and J. A. Cooper. 1986. Actin and actin-binding proteins. A critical evaluation of mechanisms and functions. *Annu. Rev. Biochem.* 55:987-1035.
- Porter, K. R. 1984. The cytomatrix: a short history of its study. *J. Cell Biol.* 99:3s-12s.
- Schliwa, M., and J. Van Blerkom. 1981. Structural interaction of cytoskeletal components. *J. Cell Biol.* 90:222-235.
- Sellen, D. B. 1983. The diffusion of compact macromolecules through biological gels. *NATO Adv. Stud. Inst.* 59:209-219.
- Simon, J. R., R. H. Furukawa, B. R. Ware, and D. L. Taylor. 1988a. The molecular mobility of  $\alpha$ -actinin and actin in a reconstituted model of gelation. *Cell Motil.* 11:64-82.
- Simon, J. R., A. Gough, E. Urbanik, F. Wang, F. Lanni, B. R. Ware, and D. L. Taylor. 1988b. Analysis of rhodamine and fluorescein-labeled F-actin diffusion in vitro by fluorescence photobleaching recovery. *Biophys. J.* 54:801-815.
- Spudich, J. A., and W. Watt. 1971. The regulation of rabbit skeletal muscle contraction. *J. Biol. Chem.* 246:4866-4871.
- Stossel, T. P., C. Chaponnier, R. M. Ezzell, J. H. Hartwig, P. A. Janmey, D. J. Kwiatkowski, S. E. Lind, D. B. Smith, F. S. Southwick, H. L. Yin, and K. S. Zaner. 1985. Nonmuscle actin-binding proteins. *Annu. Rev. Cell Biol.* 1:353-402.
- Tait, J. F., and C. Frieden. 1982. Polymerization and gelation of actin studied by fluorescence photobleaching recovery. *Biochemistry*. 21:3666-3674.
- Taylor, D. L., and J. S. Condeelis. 1979. Cytoplasmic structure and contractility in amoeboid cells. *Int. Rev. Cytol.* 56:57-144.
- Taylor, D. L., and M. Fehcheimer. 1982. Cytoplasmic structure and contractility: the solution-contraction coupling hypothesis. *Phil. Trans. R. Soc. Lond. B*. 229:185-187.
- Wang, J. H. 1954. Theory of the self-diffusion of water in protein solutions. A new method for studying the hydration and shape of protein molecules. *J. Am. Chem. Soc.* 76:4755-4765.
- Wolf, D. E. 1989. Designing, building, and using a fluorescence recovery after photobleaching instrument. *Methods Cell Biol.* 30:271-306.
- Wolosewick, J. J., and Porter, K. R. 1979. Microtrabecular lattice of the cytoplasmic ground substance. *J. Cell Biol.* 82:114-139.
- Yguerabide, J., J. A. Schmidt, and E. E. Yguerabide. 1982. Lateral mobility in membranes as detected by fluorescence recovery after photobleaching. *Biophys. J.* 39:69-75.